REGULAR ARTICLE

blood advances

Molecular mechanisms mediating relapse following ivosidenib monotherapy in *IDH1*-mutant relapsed or refractory AML

Sung Choe,[1,*] Hongfang Wang,[1,*] Courtney D. DiNardo,[2,*] Eytan M. Stein,[3] Stéphane de Botton,[4] Gail J. Roboz,[5] Jessica K. Altman,[6] Alice S. Mims,[7] Justin M. Watts,[8] Daniel A. Pollyea,[9] Amir T. Fathi,[10] Martin S. Tallman,[3] Hagop M. Kantarjian,[2] Richard M. Stone,[11] Lynn Quek,[12] Zenon Konteatis,[1] Lenny Dang,[1] Brandon Nicolay,[1] Parham Nejad,[1] Guowen Liu,[1] Vickie Zhang,[1] Hua Liu,[1] Meredith Goldwasser,[1] Wei Liu,[1] Kevin Marks,[1] Chris Bowden,[1] Scott A. Biller,[1] Eyal C. Attar,[1,†] and Bin Wu[1,†]

[1]Agios Pharmaceuticals, Inc., Cambridge, MA; [2]University of Texas MD Anderson Cancer Center, Houston, TX; [3]Memorial Sloan Kettering Cancer Center, New York, NY; [4]Department of Hematology, Institut Gustave Roussy, Villejuif, France; [5]Weill Cornell Medicine/New York-Presbyterian Hospital, New York, NY; [6]Robert H. Lurie Comprehensive Cancer Center, Northwestern University, Chicago, IL; [7]The Ohio State University Wexner Medical Center, Columbus, OH; [8]Sylvester Comprehensive Cancer Center, University of Miami, Miami, FL; [9]Division of Hematology, University of Colorado School of Medicine, Aurora, CO; [10]Massachusetts General Hospital, Harvard Medical School, Boston, MA; [11]Dana-Farber Cancer Institute, Boston, MA; and [12]Medical Research Council Molecular Hematology Unit, Weatherall Institute of Molecular Medicine, University of Oxford, Oxford, United Kingdom

Key Points

- Baseline mutations are associated with response (*JAK2*) or resistance (*NRAS*, *PTPN11*) to ivosidenib monotherapy in m*IDH1* R/R AML.
- 2-HG restoration via novel *IDH1* second-site and *IDH2* mutations, and non-*IDH*–related pathways, are identified at relapse.

Isocitrate dehydrogenase (*IDH*) 1 and 2 mutations result in overproduction of D-2-hydroxyglutarate (2-HG) and impaired cellular differentiation. Ivosidenib, a targeted mutant IDH1 (mIDH1) enzyme inhibitor, can restore normal differentiation and results in clinical responses in a subset of patients with m*IDH1* relapsed/refractory (R/R) acute myeloid leukemia (AML). We explored mechanisms of ivosidenib resistance in 174 patients with confirmed m*IDH1* R/R AML from a phase 1 trial. Receptor tyrosine kinase (RTK) pathway mutations were associated with primary resistance to ivosidenib. Multiple mechanisms contributed to acquired resistance, particularly outgrowth of RTK pathway mutations and 2-HG–restoring mutations (second-site *IDH1* mutations, *IDH2* mutations). Observation of multiple concurrent mechanisms in individual patients underscores the complex biology of resistance and has important implications for rational combination therapy design. This trial was registered at www.clinicaltrials.gov as #NCT02074839

Introduction

Somatic mutations in the genes encoding the metabolic enzymes isocitrate dehydrogenase (IDH) 1 and 2 are found in multiple solid and hematologic tumors, including acute myeloid leukemia (AML). The altered enzymes have gain-of-function activity, catalyzing the reduction of α-ketoglutarate to the oncometabolite D-2-hydroxyglutarate (2-HG).[1,2] Accumulation of 2-HG results in metabolic dysregulation and inhibition of α-ketoglutarate-dependent enzymes, which drive oncogenesis via epigenetic dysregulation and a block in cellular differentiation.[3-5] Mutations in *IDH1* and *IDH2* are present in 6% to 10%[2,6-8] and 9% to 13%[8,9] of patients with AML, respectively, and *IDH1* mutations have been associated with poor clinical outcomes in patients with AML.[10-12]

The mutant IDH (mIDH) inhibitors ivosidenib (Tibsovo; Agios Pharmaceuticals, Inc.; formerly AG-120)[13] and enasidenib (Idhifa; Celgene Corp.; formerly AG-221)[14] are targeted, allosteric inhibitors of the mIDH1 and mIDH2 enzymes, respectively. Both are approved in the United States for the treatment of adults with relapsed or refractory (R/R) AML with an *IDH1* or *IDH2* mutation, respectively, as detected by a test approved by the US Food and Drug Administration, and ivosidenib is approved for patients with m*IDH1* newly diagnosed AML who are at least 75 years of age or who have comorbidities that preclude the use of intensive chemotherapy.[15,16] Pharmacologic engagement of the mIDH1/2 protein by the

Submitted 15 January 2020; accepted 18 March 2020; published online 7 May 2020.
DOI 10.1182/bloodadvances.2020001503.

*S.C., H.W., and C.D.D. are joint first authors.

†E.C.A. and B.W. are joint senior authors.

Investigators interested in data sharing and collaboration should contact the corresponding author, Bin Wu, at bin.wu@agios.com.

The full-text version of this article contains a data supplement.

respective inhibitor results in lowering of 2-HG levels in most treated patients. However, with both mIDH inhibitors, the proportion of patients in whom 2-HG is reduced exceeds the proportion of patients achieving clinical response, indicating that 2-HG reduction alone is not sufficient for a response.[17,18]

Therapeutic resistance to mIDH1/2 inhibitors has implications for treatment and the development of rational combination regimens, but mechanisms of primary and secondary resistance to these inhibitors are not yet well understood. Preliminary analyses of co-occurring mutations at baseline, defined as the most recent measurement before the first administration of ivosidenib, have found that certain co-occurring mutations are associated with primary resistance. Baseline mutations in receptor tyrosine kinase (RTK) pathway genes were more common in patients with m*IDH1* R/R AML who did not achieve complete remission (CR) or CR with partial hematologic response (CRh) with ivosidenib treatment.[17] In m*IDH2* R/R AML treated with enasidenib, significantly fewer patients with *NRAS* mutations achieved CR.[18] Secondary resistance after a clinical response to enasidenib was associated with the emergence of AML-related mutations, such as *RUNX1* and *FLT3*,[19] and *IDH*-related mutations, including outgrowth of m*IDH1* in patients who initially had m*IDH2* (isoform switching),[19,20] and the emergence of second-site *IDH2* mutations.[21] However, these reports were based on a limited number of patients, and the frequency and breadth of resistance mechanisms have not been comprehensively characterized.

To fully characterize the mechanisms of response and relapse to ivosidenib monotherapy, we conducted a comprehensive genomic analysis of samples from a large cohort of patients with m*IDH1* R/R AML treated in a phase 1 study[17] whose starting dose of ivosidenib was the approved dose of 500 mg once daily (QD). Here, we confirm that RTK pathway mutations are associated with primary resistance to ivosidenib. Importantly, we found that multiple mechanisms contribute to relapse after ivosidenib therapy, including emergence or outgrowth of AML-related mutations, such as RTK pathway genes, and *IDH*-related mutations (comprising second-site mutations in *IDH1* and mutations in *IDH2)*, which were associated with increased 2-HG. These various mechanisms of resistance occurred in isolation or in combination, underscoring the complex biology of treatment resistance.

Methods

Study design

The design of this phase 1, multicenter, open-label, dose-escalation and dose-expansion study of ivosidenib in patients with m*IDH1* advanced hematologic malignancies (ClinicalTrials.gov number: NCT02074839) has been reported elsewhere, along with eligibility criteria.[17] Patients received ivosidenib orally QD in 28-day cycles (supplemental Methods).

Biomarker analysis methods are reported in the supplemental Methods.

Results

Patient cohort

A total of 179 patients with R/R AML were enrolled and treated with a starting dose of 500 mg QD in the first-in-human, open-label, dose-escalation and dose-expansion trial of ivosidenib in patients with m*IDH1* advanced hematologic malignancies; follow-up is ongoing.[17] The current analysis focused on the subset of 174 patients with R/R AML with m*IDH1* confirmation, using the Abbott RealTime IDH1 assay. The baseline demographic characteristics are summarized in supplemental Table 1. The number of patients included in each of the different molecular analyses reported here is shown in Figure 1.

Baseline comutations in RTK pathway genes are associated with primary treatment resistance

Co-occurring mutation profiling was performed on whole bone marrow by next-generation sequencing (NGS; detection sensitivity, 1%-5%). Per patient co-occurring mutations at baseline (n = 167), organized by best overall response category, are shown in Figure 2A. The subset of 101 patients whose baseline mutational profiles were reported previously[17] are all included in this analysis. The most frequent oncogenic co-occurring mutations detected at baseline were *DNMT3A* (35%), *NPM1* (26%), *SRSF2* (24%), *ASXL1* (18%), *RUNX1* (18%), *NRAS* (14%), and *TP53* (13%; see supplemental Table 2 for full list of genes tested). Among 11 patients with mutations in *FLT3*, 2 were internal tandem duplications, and 9 were in the tyrosine kinase domain (TKD) or juxtamembrane domain point mutations. There were 14 patients with mutations in *TET2* at baseline. The mean number of mutations (including m*IDH1*) as an estimate of genomic complexity was lower in patients achieving CR or CRh responses (2.8) than in patients with non-CR/CRh responses and nonresponders (3.7), with $P < .001$ (Student *t* test; supplemental Figure 2). RTK pathway mutations, along with an increased number of mutations, are similarly associated with primary treatment resistance to enasidenib in m*IDH2* R/R AML.[18]

Baseline mutations in the individual RTK pathway genes of *NRAS* and *PTPN11*, and in the RTK pathway genes as a group (defined in this analysis as *NRAS*, *KRAS*, *PTPN11*, *KIT*, and *FLT3*), were associated with a significantly lower likelihood of achieving a best response of CR or CRh with ivosidenib ($P = .004$, $P = .016$, and $P < .001$, respectively; Fisher's exact test; Figure 2B), suggesting a role in primary treatment resistance. Nevertheless, CR or CRh was observed in 2 (9%) of 23 patients with baseline *NRAS* mutations (see single-cell DNA sequencing analyses for further details). Responses were also observed in patients with mutations in genes associated with adverse prognosis,[22] including *ASXL1* (10 of 30; 33%), *RUNX1* (9 of 30; 30%), and *TP53* (5 of 21; 24%). In addition, 7 (64%) of 11 patients with baseline *JAK2* V617 mutations, which are commonly observed in patients with myeloproliferative neoplasms and secondary AML with a history of myeloproliferative neoplasms, achieved CR (n = 6) or CRh (n = 1; $P = .05$; Figure 2B). Two patients with baseline *FLT3*-TKD mutations achieved CR. No significant association was seen between response and mutations in other genes tested (see supplemental Table 2 for full list).

Clinical response is not predicted by the position of m*IDH1* within the clonal hierarchy

We previously demonstrated that in 101 patients with m*IDH1* R/R AML who received ivosidenib in the phase 1 study, there was no significant difference in baseline m*IDH1* variant allele frequency (VAF) between CR or CRh responders and those with other responses or no response.[17] The lack of significant correlation was also observed in this larger data set of 167 patients ($P = .087$;

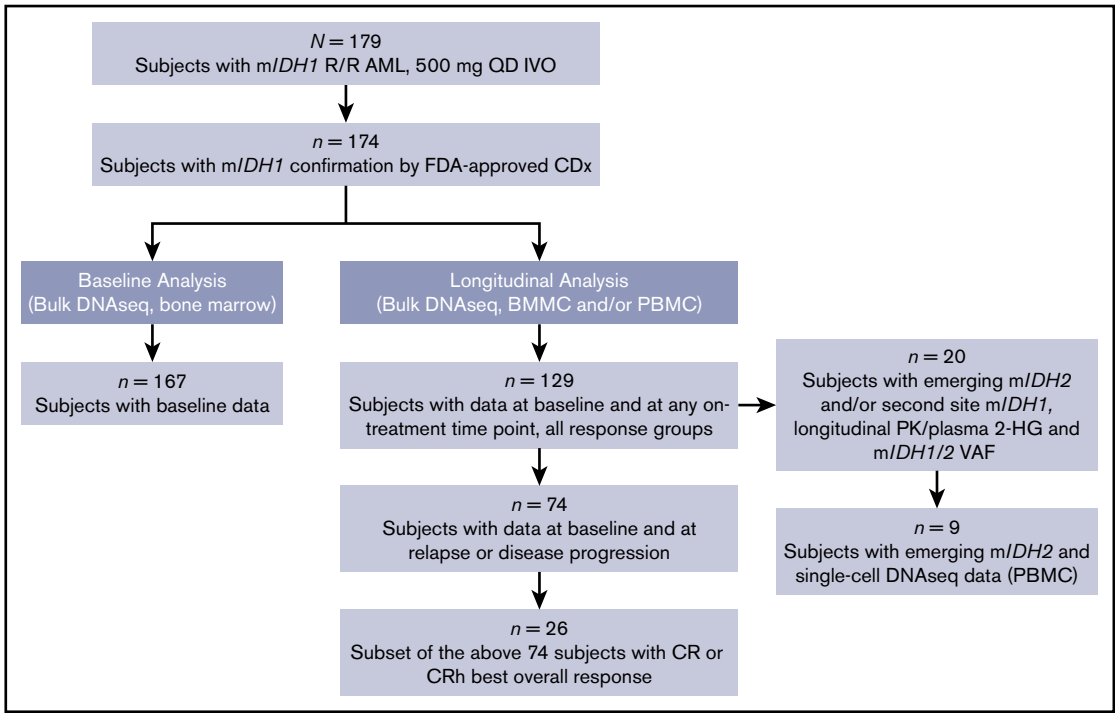

Figure 1. Patient flow diagram summarizing analysis sets. Analyses did not include all patients treated in this population because of several factors, including lack of complete sample availability for all protocol-designated time points and/or suboptimal quantity and/or quality of some samples, resulting in failure to obtain valid data. BMMC, bone marrow mononuclear cell; CDx, companion diagnostic test; DNAseq, DNA sequencing; FDA, US Food and Drug Administration; IDH, isocitrate dehydrogenase; IVO, ivosidenib; PBMC, peripheral blood mononuclear cell; PK, pharmacokinetics; VAF, variant allele frequency.

Fisher's exact test), with m*IDH1* VAF in whole bone marrow ranging from 3% to 58%, as measured by NGS (supplemental Figure 3). Response was observed in patients with lower m*IDH1* VAF. For example, among 18 patients with m*IDH1* VAF of 10% or less, 7 achieved CR or CRh.

In the present analysis, we investigated the position of m*IDH1* in the clonal hierarchy by examining the baseline VAF of co-occurring gene mutations in relation to m*IDH1* in bone marrow samples, as well as the association with clinical response. m*IDH1* was defined as subclonal in a sample if any comutation VAF was greater than m*IDH1* VAF +5%; otherwise, it was defined as clonal. The 5% cutoff was selected based on the distribution of VAFs in replicate samples on this NGS platform,[23] and this cutoff was also used by Molenaar et al.[24] Details on the manual curation steps that were taken to refine this analysis are provided in the supplemental Methods.

In this data set, m*IDH1* was subclonal in 28% of patients and clonal in 72% (Figure 3A). There was no association between clonal or subclonal m*IDH1* status and achieving a best response of CR or CRh ($P = 1.000$; Fisher's exact test). Mutations in *SRSF2*, *ASXL1*, *JAK2*, *TET2*, *U2AF1*, *BCOR*, and *DNMT3A* occurred more frequently with higher VAF than m*IDH1*, whereas mutant *NRAS*, *NPM1*, *PTPN11*, *PHF6*, *RUNX1*, *STAG2*, and *FLT3* VAFs were more frequently lower than m*IDH1* VAF (Figure 3B). Other groups have reported that mutations in RTK pathway genes generally occur later in clonal evolution than mutations in *IDH1/2*.[25] Baseline m*IDH1* VAF in relation to other gene mutations is shown in supplemental Figure 4.

Relapse is characterized by multiple mechanisms, including emergence of RTK pathway mutations and 2-HG–restoring mutations

We performed longitudinal bulk NGS on bone marrow mononuclear cells and/or peripheral blood mononuclear cells to characterize the mutational profile both at baseline and at the time of relapse or disease progression. Longitudinal data were available for 129 patients with samples at baseline and at least 1 on-treatment point irrespective of response (see supplemental Table 3 for all mutations newly identified during treatment). Of these patients, data were available for 74 patients at relapse (after CR, CRh, CR with incomplete hematologic recovery, CR with incomplete platelet recovery, or morphologic leukemia-free state) or at disease progression (for patients with best overall response of stable disease or progressive disease), and the mutational profile of these 74 patients at relapse or progression was compared with the mutational profile at baseline (Figure 4A).

Mutations identified by bulk NGS at the time of relapse/progression, but not detected at baseline, were categorized as either AML related or *IDH* related (2-HG restoring). Mutations in RTK pathway genes (*NRAS*, *KRAS*, *PTPN11*, *KIT*, *NF1*, *BRAF*, or *FLT3*) were identified in 20 (27%) of 74 patients; *IDH*-related mutations occurred at a similar frequency (17 of 74; 23%) and included second-site mutations in *IDH1* (10 of 74; 14%) and canonical mutations in *IDH2* (9 of 74; 12%; Figure 4B). *IDH2* mutations and second-site *IDH1* mutations were not mutually exclusive (ie, both were observed in 2 patients). In the 26 patients with best response of CR/CRh who relapsed, *IDH*-related mutations emerged at

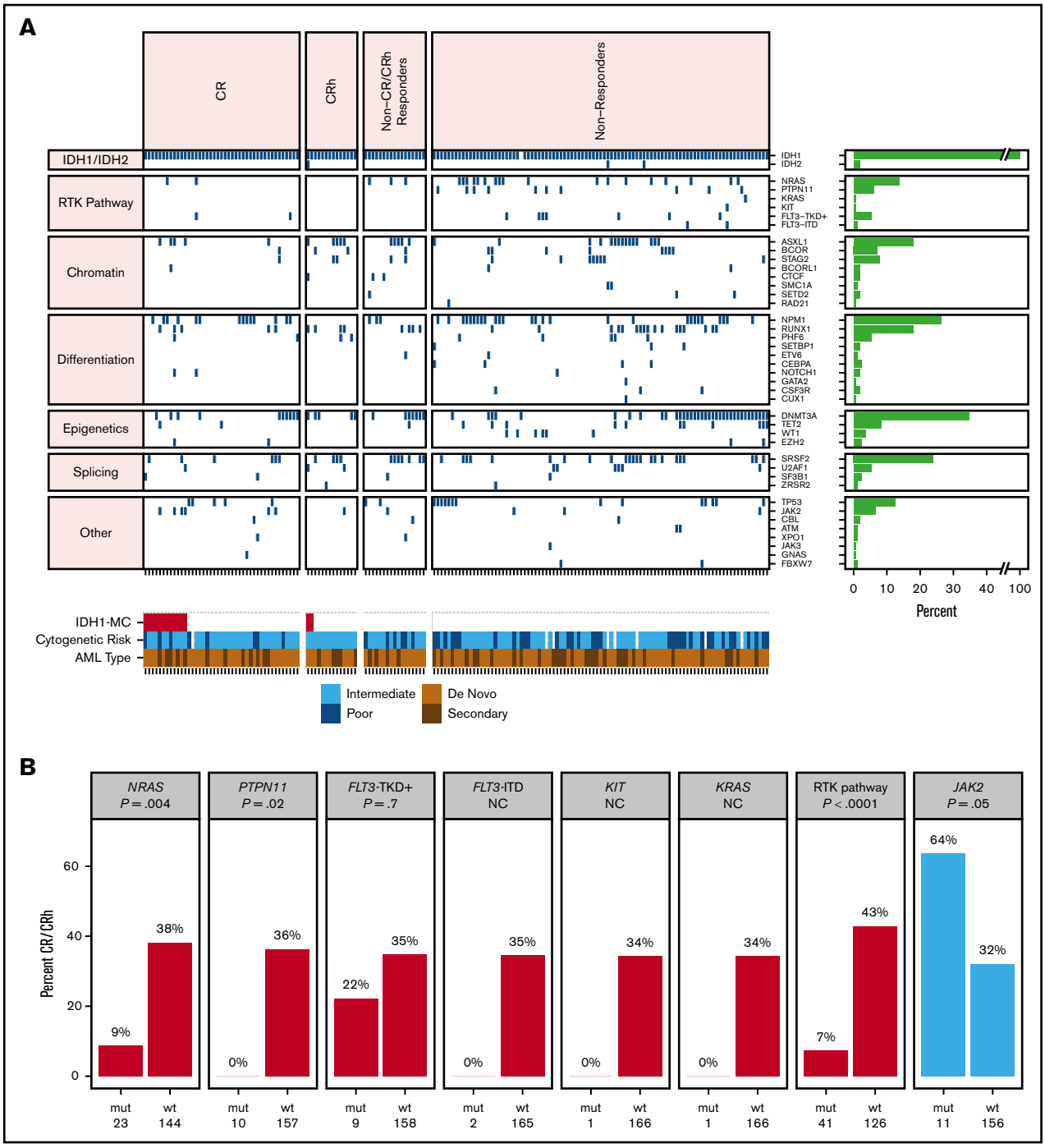

Figure 2. Baseline co-occurring mutation analysis. (A) Heat map showing co-occurring mutations at baseline by best overall response category (NGS; whole bone marrow; n = 167 patients). Merge of dose-escalation and dose-expansion data (VAF cutoff, 1%-5%). Cytogenetic risk was classified according to the National Comprehensive Cancer Network Clinical Practice Guidelines for AML, version 1.2015. The bar graph depicts the frequency of genes with co-occurring mutations. A similar heat map with detected mutations by VAF level is provided in supplemental Figure 1. (B) Association between mutation status and best response. *P* value is based on Fisher's exact test examining the association between specific pathway or gene mutations and best overall response of CR/CRh vs non-CR/CRh responders and nonresponders. NC denotes *P* value not calculated because of small number of patients with mutation. FLT3-TKD^{+} denotes FLT3-TKD or juxtamembrane domain point mutations. Data source: 167 patients with baseline NGS data from whole bone marrow. IDH1-MC, *IDH1* mutation clearance; ITD, internal tandem duplication; mut, mutant; wt, wild-type.

a similar frequency (35%) as RTK pathway genes. Notably, 5 patients had newly identified mutations in both RTK pathway genes and *IDH1* and/or *IDH2* at relapse/progression.

Bulk NGS data showed that second-site *IDH1* mutations and *IDH2* mutations were rare at baseline, occurring in 4 (2.4%) of 167 patients with baseline bone marrow DNA profiling. Of these, 1

A

m*IDH1* status	n (%)	CR/CRh best response, n (%)
Clonal	119 (72)	41/119 (34)
Subclonal	47 (28)	16/47 (34)
Total	166	

B

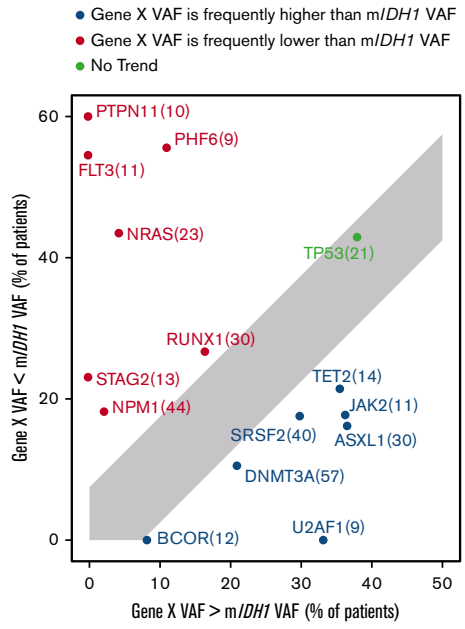

Figure 3. Clonal hierarchy of m*IDH1* and co-occurring mutations. (A) Association of clinical response and m*IDH1* clonal/subclonal status. m*IDH1* was defined as subclonal in a sample if any comutation VAF was greater than m*IDH1* VAF +5%; otherwise, it was defined as clonal. See details in the supplemental Methods. (B) Plot showing the tally of how often a co-occurring gene VAF is observed to be lower (red) or higher (blue) than m*IDH1* VAF by NGS. Only genes that were mutated in at least 5% of patients are shown. Per-gene VAFs are detailed in supplemental Figure 4. For each gene X, the subset of patients with a mutation in gene X is selected (n in parentheses) and plotted, with the x-axis showing the percentage of patients where gene X VAF > m*IDH1* VAF +5% and the y-axis showing the percentage of patients where gene X VAF < m*IDH1* VAF −5%.

patient had 2 second-site mutations in *IDH1* (R119P and G131A) and had previously received treatment with the m*IDH1* inhibitor IDH305. Three (1.8%) patients had m*IDH2*-R140 at screening. In contrast, 41 (25%) of 167 patients had RTK pathway mutations at screening.

The second-site *IDH1* mutations that emerged during treatment with ivosidenib monotherapy included the previously described m*IDH1*-S280F in addition to 5 novel, previously unidentified mutations (Figure 5A; supplemental Table 4). Although no dominant second-site *IDH1* mutation was detected in this data set, the second-site *IDH1* mutations clustered into 2 subregions of the IDH1 protein. Notably, all *IDH2* mutations that emerged during treatment were R140Q in this R/R AML data set (supplemental Table 4). However, emergence of *IDH2*-R172K was observed in 1 patient with newly diagnosed AML in the phase 1 study (data on file).

The majority of the newly identified second-site *IDH1* and *IDH2* mutations (15 of 16 with available 2-HG data at relapse) were associated with a concurrent increase in 2-HG levels, and are thus termed 2-HG–restoring mutations (see details in supplemental Figure 5).

Structural and biochemical characterization of second-site IDH1 mutations

IDH1/2 mutations in AML that lead to the generation of 2-HG localize to the active sites of the enzymes, on residues R132 in IDH1 and R140 or R172 in IDH2.[1,2] Ivosidenib and enasidenib bind to allosteric sites, thus stabilizing the open, inactive conformation of the enzymes.[14] The crystal structure model of IDH1-R132H in open conformation (when ivosidenib or an analog is bound) is shown in Figure 5B, indicating the active site with the cofactor NADPH and the location of the inhibitor in the allosteric, tetra-helical binding site. We performed 3-dimensional modeling of second-site IDH1 mutations using an analog of ivosidenib (AGI-14686; supplemental Figure 6A) to determine whether ivosidenib binding would be affected by these mutations. The model (see supplemental Methods for development) placed AGI-14686 in the tetra-helical center of the dimeric IDH1-R132H protein and allowed us to observe the second-site IDH1 mutations, all of which could be predicted to affect ivosidenib and/or cofactor binding. Two groups of mutations were postulated: those directly affecting the drug-binding pocket or NADPH cofactor/active sites and those that indirectly affect either the ivosidenib binding site or the cofactor/substrate site. The binding model for the IDH1-R132H-S280F mutation (Figure 5C) places the di-F cyclopentane group of the inhibitor near Ser280 within the binding pocket of the protein. Mutation of Ser280 to Phe creates a steric interference with ivosidenib (and its analogs), and thus prevents binding. The binding model for the IDH1-R119P mutation is shown in supplemental Figure 6B. This mutation is located on the protein loops covering the ivosidenib binding site; the proline-induced changes in backbone conformation and rigidity of the mIDH1 protein are predicted to alter the kinetics of ivosidenib binding. Modeling of additional second-site IDH1 mutations predicts that they would affect ivosidenib or NADPH binding either directly or indirectly (supplemental Figure 6C-F). Biochemical characterization of both IDH1-S280F and IDH1-R119P second-site mutations confirms loss of ivosidenib inhibitory potency (Figure 5D). At steady state, the free maximum and average plasma concentrations of ivosidenib are found to be 0.94 and 0.71 μM, respectively, given the mean percentage plasma protein binding of 91.6%.[15,26] This level exceeds the IC_{50} of pathogenic IDH1-R132 mutants, but is below that of the IDH1-R132C-S280F double mutant, and is within close range of that of the IDH1-R132C/L-R119P mutant in the in vitro setting, suggesting that the level of ivosidenib in plasma is not sufficient to inhibit the second-site mutation. There were no differences in plasma 2-HG elevations at relapse or progression, irrespective of the nature of the second-site mutations (supplemental Figure 5).

Single-cell DNA sequencing analyses reveal complex polyclonal resistance mechanisms

To assess clonal architecture heterogeneity and dynamics in the relapse setting at single-cell resolution with greater precision than is afforded by NGS, we conducted single-cell DNA sequencing analyses (Tapestri Platform; Mission Bio; 19-gene AML panel) on

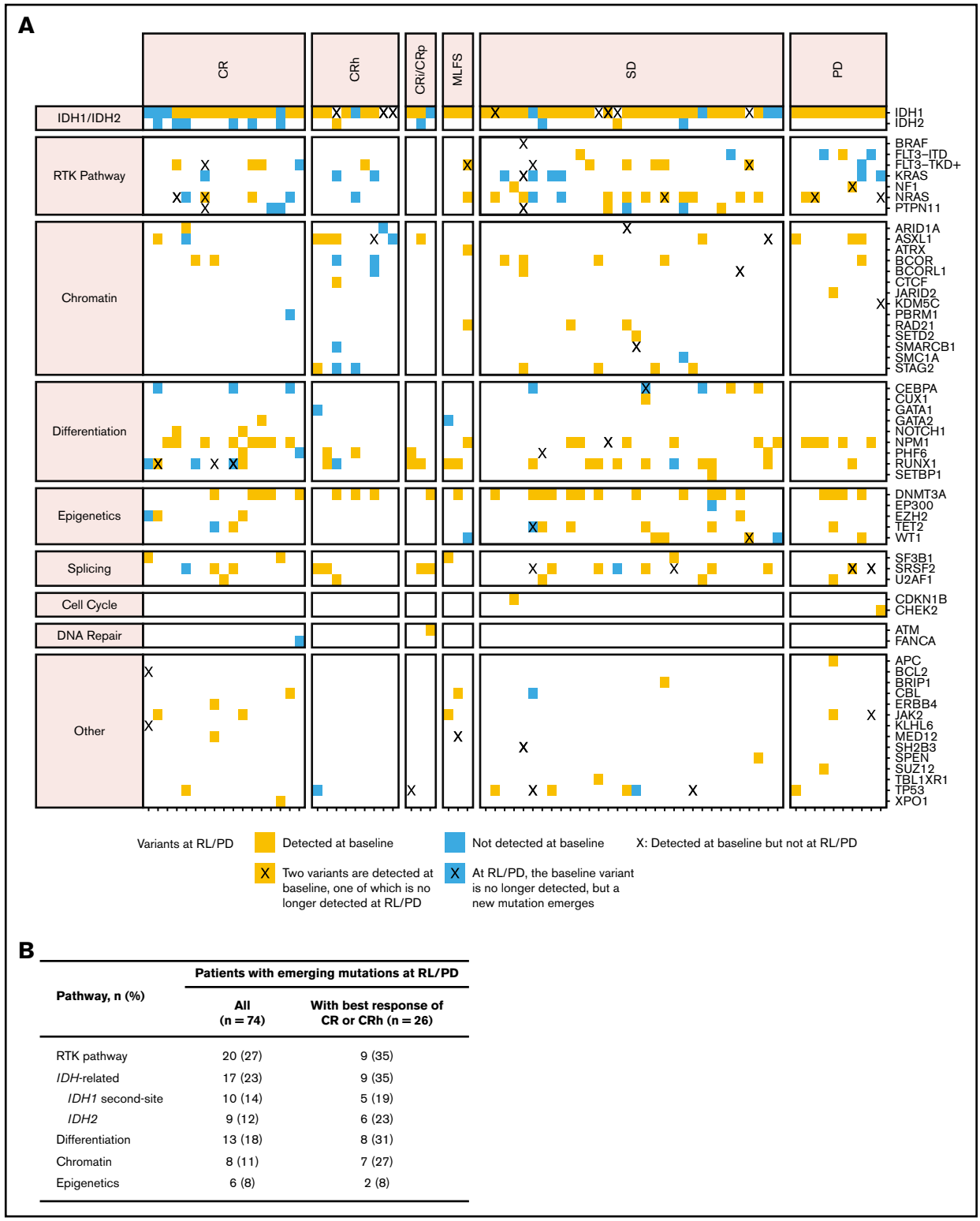

B

Pathway, n (%)	Patients with emerging mutations at RL/PD	
	All (n = 74)	With best response of CR or CRh (n = 26)
RTK pathway	20 (27)	9 (35)
IDH-related	17 (23)	9 (35)
IDH1 second-site	10 (14)	5 (19)
IDH2	9 (12)	6 (23)
Differentiation	13 (18)	8 (31)
Chromatin	8 (11)	7 (27)
Epigenetics	6 (8)	2 (8)

Figure 4. Mutations in genes and pathways detected at relapse and progression. (A) Gene mutations detected at relapse/progressive disaease (RL/PD) in patients with paired baseline and RL/PD data (n = 74), with genes organized by pathway and patients sorted by best overall response. Blue squares indicate new mutations at RL/PD that were not detected at baseline. Blue squares in the *IDH1* mutation row indicate emergent second-site *IDH1* mutations at time of RL/PD. Orange squares indicate mutations identified at RL/PD that were also detected at baseline. An X indicates that a variant in that gene that was detected at baseline is no longer detected at relapse. (B) Frequency of emergence of mutations by pathway in patients with data at baseline and at RL/PD (n = 74). CRi, complete remission with incomplete hematologic recovery; CRp, complete remission with incomplete platelet recovery; MLFS, morphologic leukemia-free state; SD, stable disease.

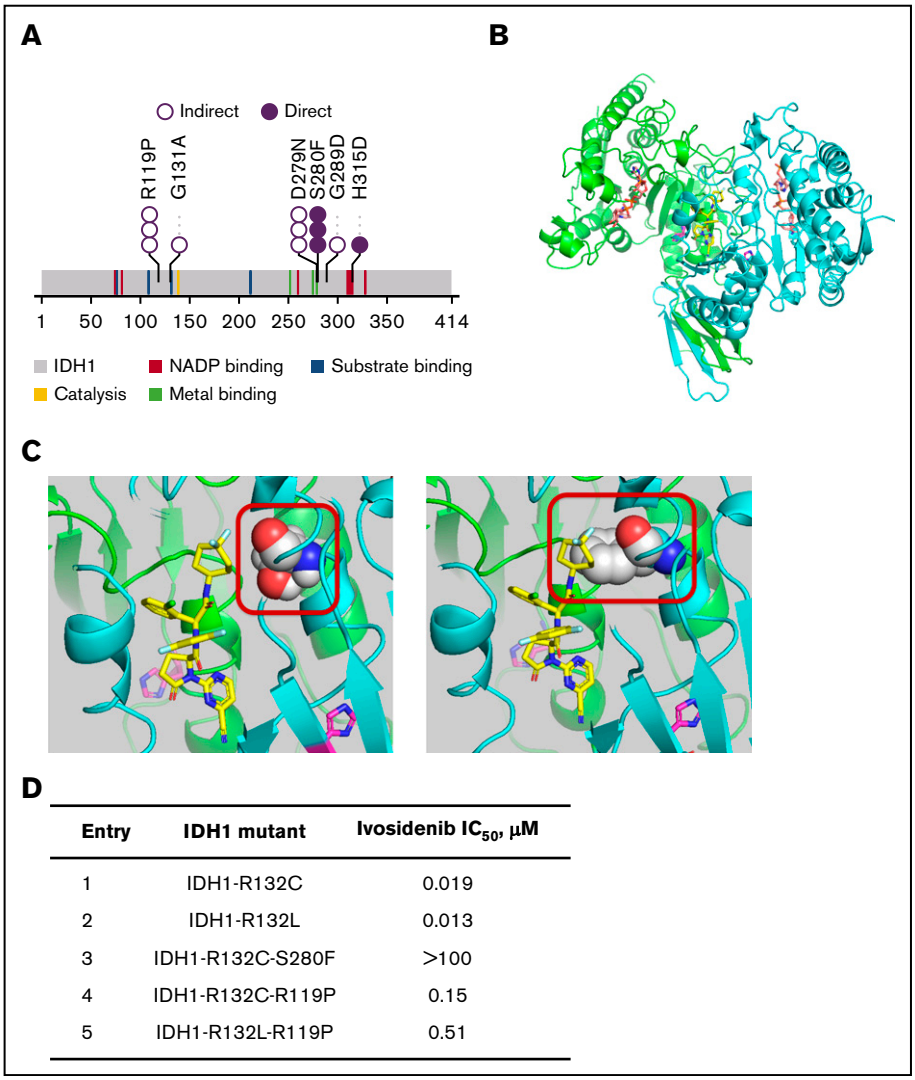

Entry	IDH1 mutant	Ivosidenib IC_{50}, μM
1	IDH1-R132C	0.019
2	IDH1-R132L	0.013
3	IDH1-R132C-S280F	>100
4	IDH1-R132C-R119P	0.15
5	IDH1-R132L-R119P	0.51

Figure 5. 2-HG–restoring mutations emerging at relapse or disease progression. (A) Second-site *IDH1* mutations emerging during ivosidenib treatment (n = 20). Each circle represents a single patient with detection of the mutation. Direct denotes that the mutation makes contact with the ivosidenib or cofactor (NADPH) binding pocket by 3-dimensional modeling. Indirect denotes that it induces structural changes in vicinity of ivosidenib or cofactor binding pockets (hypothesized). Novel mutations (not previously published) are mostly the indirect type. (B) Crystal structure of IDH1-R132H in the inactive, open conformation. The cocrystal structure of IDH1-R132H with inhibitor 20a (PBD accession no. 5L57)[40] was obtained at 2.7 A° resolution and used to develop the model for the ivosidenib analog AGI-14686 (supplemental Methods). The homodimeric protein structure is shown with the inhibitor (AGI-14686) in yellow, occupying the middle of the tetra-helical domain. The protein monomers are shown in green and cyan, the mutated 132H residue in magenta and cofactor NADPH in orange. (C) The mIDH1-AGI-14686 binding model for the IDH1-R132H-S280F mutation places the di-F cyclopentane of AGI-14686 near Ser280 (left). Mutation of Ser280 to Phe (right) will create a steric interference with ivosidenib (or its analogs), and thus will no longer bind to mIDH1. The mIDH1 protein is depicted in cartoon (green and blue for each monomer), the ivosidenib analog AGI-14686 in yellow sticks, and residue 280 in spheres (Ser in the left panel, Phe in the right panel). R132H is shown in magenta. (D) Biochemical 50% inhibitory concentration (IC_{50}) for second-site IDH1 mutations. We expressed various combinations of IDH1 mutants with second-site mutations and examined biochemically whether they were still inhibited by ivosidenib.

matched baseline and relapse peripheral blood mononuclear cell sample pairs from 9 patients who had a response to ivosidenib followed by emergence of m*IDH2*. The polyclonal relapse mechanisms were grouped into the following 3 categories: 6 of 9 patients had no detectable m*IDH2* at baseline, but m*IDH2* was identified in the same clone as m*IDH1* at relapse (Figure 6A; elevated 2-HG observed at relapse); 1 of 9 patients had no detectable m*IDH2* at baseline, but m*IDH2* was identified in a separate clone than m*IDH1* at relapse (isoform switching; Figure 6B); and 2 of 9 patients had detectable m*IDH2* at baseline in a separate clone than m*IDH1* (Figure 6C). Figure 6A represents the clonal architecture of AML in a patient with 2 distinct m*IDH1* clones at baseline: 1 harboring *NPM1*/*NRAS* comutations and the other harboring *NPM1*/*FLT3*-TKD comutations. After ivosidenib treatment, the *IDH1*/*NPM1*/*NRAS* clone was no longer detected. Reduction in the *IDH1*/*NPM1*/*FLT3*-TKD clone was observed at cycle 2 day 1, but it ultimately expanded at relapse with the acquisition of m*IDH2*. Figure 6B demonstrates the clonal architecture in a patient without m*IDH2* at baseline. Emergence of m*IDH2* in a separate clone than m*IDH1* was observed at cycle 12 day 1

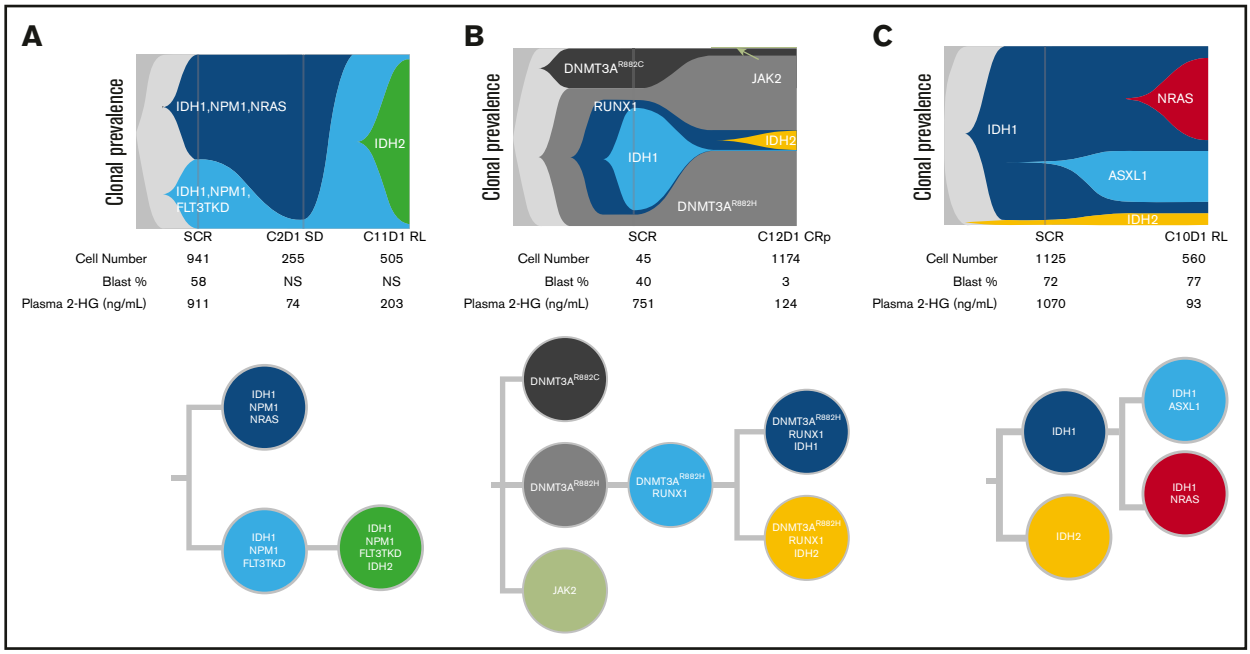

Figure 6. Polyclonal relapse mechanisms. Single-cell analysis showing clonal evolution in individual patients. (A) m*IDH2* acquired in the same clone as m*IDH1*, with elevation of 2-HG at relapse. Two distinct m*IDH1* clones were present at baseline: 1 harboring *NPM1*/*NRAS* and the other harboring *NPM1*/*FLT3*-TKD comutations. After ivosidenib treatment, the *IDH1*/*NPM1*/*NRAS* clone was no longer detected. Reduction in the *IDH1*/*NPM1*/*FLT3*-TKD clone was observed at cycle 2 day 1, but it ultimately expanded at relapse with the acquisition of m*IDH2*. (B) m*IDH2* was not detected at baseline, but emergence of m*IDH2* in a separate clone than m*IDH1* was observed at cycle 12 day 1, with elevation of 2-HG. (C) m*IDH2* was present at baseline (though not detected by bulk NGS) in a distinct clone to m*IDH1*, with clinical relapse associated with detection of an *NRAS* clone. In this case of *NRAS*-driven clinical relapse, the 2-HG levels remained low at relapse. Additional details on these cases shown in supplemental Figure 7. NS, not specified.

with elevated 2-HG. Figure 6C shows a case in which m*IDH2* was present at baseline by single-cell DNA sequencing, but not detected by bulk NGS, with relapse most likely a result of acquisition of *NRAS* mutation in the m*IDH1* clone and/or expansion of the *IDH1*/*ASXL1* clone, as 2-HG remained low at relapse. These findings show that relapse occurs as a result of expansion of multiple parallel clones spanning different pathways. Furthermore, phylogenetic tree reconstruction from clonotypes indicated patterns of both branching and linear clonal evolution. Additional cases are provided in supplemental Figure 7.

Discussion

We report a comprehensive analysis of primary and secondary mechanisms of resistance to ivosidenib monotherapy in patients with m*IDH1* R/R AML. The bulk NGS and single-cell sequencing results highlight the polyclonal nature of AML and illustrate the complex cellular and molecular mechanisms that drive clinical relapse in the setting of ivosidenib treatment. Mutations in RTK pathway genes were associated with primary treatment resistance in this population and were a frequent secondary resistance mechanism. Interestingly, *KRAS* mutations were more frequent at relapse/progression than at baseline. In addition, 2-HG restoration as a result of mutations preventing drug/cofactor binding and/or emergence of an *IDH2* mutation represents a mechanism of secondary resistance, emerging at a similar frequency as RTK pathway mutations.

We previously reported an association between baseline mutations in RTK pathway genes and primary resistance to ivosidenib.[17] With a larger data set, we now observe significant associations between single RTK pathway genes (*NRAS*, *PTPN11*) and best overall response. This finding is consistent with previous work showing an association between *NRAS* mutation and a lower likelihood of response to enasidenib in patients with m*IDH2* R/R AML.[18] However, in the present study, CR was observed in 2 of 23 patients with *NRAS* mutations, indicating that these mutations at baseline do not confer universal resistance. This is supported by our single-cell DNA sequencing analyses, which revealed an example of a clone harboring an *NRAS* mutation (along with *IDH1 and NPM1* comutations) that was no longer detected after ivosidenib treatment.

The results from this large data set also extend the findings of earlier isolated case studies, which revealed 2-HG–restoring mutations (including isoform switching and the emergence of m*IDH1*-S280F) to be mechanisms involved in secondary resistance to ivosidenib.[20,21] In our data set, the frequent observation of 2-HG–restoring mutations at relapse after CR or CRh by virtue of mutations in *IDH2* and second-site mutations in *IDH1* (9 of 26 patients; 35%) highlights the key role of 2-HG production in m*IDH1* AML. Further, single-cell DNA sequencing analyses revealed multiple instances in which m*IDH2* was not detectable at baseline, but emerged within the same clone as m*IDH1*, suggesting the existence of a selective pressure to reestablish 2-HG even in the presence of other AML driver mutations. In other single-cell DNA sequencing profiles, m*IDH2* was observed in an independent subclone, with an unknown effect on coexisting m*IDH1* clones or clinical disease features. It is possible that 2-HG production and release by these m*IDH2* subclones can affect all

leukemic and/or stromal cells in a paracrine manner. Reports indicate that 2-HG can enter specific cell types (eg, tumor-associated immune cells), potentially leading to immunosuppression.[27-30] The emergence of multiple second-site *IDH1* mutations with no dominant mutation supports the use of mIDH1 inhibitors in combination with other therapies to reduce the likelihood of resistance.

Although 2-HG–restoring mutations are a major pathway of secondary resistance, other 2-HG-independent pathways are important and may be dominant over 2-HG restoration in some cases. McMahon et al.[31] observed that reactivation of RTK pathway signaling was a major mechanism of secondary resistance to the FLT3 inhibitor gilteritinib, including the emergence of *RAS* mutations in *FLT3*-mutated subclones. We show that in addition to being associated with primary resistance, RTK pathway mutations are also associated with secondary resistance to ivosidenib monotherapy in this study population. Among patients who relapsed after achieving CR or CRh, RTK pathway mutations emerged at relapse in 9 (35%) of 26 patients. The biological processes explaining the association between RTK pathway mutations and both primary and secondary resistance to ivosidenib are not currently understood. Several hypotheses are possible. First, it may be that the proliferative and prosurvival effects of RTK pathway activation are sufficiently strong oncogenic signals to reduce dependency on 2-HG. Second, it is possible that RTK pathway-activating mutations contribute to a differentiation block that remains enforced after initiation of ivosidenib treatment. Some reports have shown that FLT3 inhibitors induce granulocytic differentiation and differentiation syndrome symptoms in some patients with *FLT3*-mutated AML.[32,33] Thus, the combination of mIDH inhibitors with RTK pathway inhibitors, including FLT3 inhibitors, may present a rational treatment strategy. A third hypothesis is that *IDH1/2* mutations result in activation of some components of RTK signaling, which would not be reversed by ivosidenib in cases with co-occurring RTK pathway mutations. In glioma, *IDH1* mutations were reported to increase platelet-derived growth factor receptor α expression levels by methylation and inactivation of a nearby CCCTC-binding factor insulator site.[34] Others have observed increased AKT/mTOR signaling in m*IDH1* cells.[35-37]

An interesting observation is that RTK pathway mutations are associated with ivosidenib resistance despite being predominantly subclonal to m*IDH1*. Our longitudinal data show that RTK pathway mutation VAFs usually increase at relapse, but they do not generally become the dominant clone. Analogously, the FLT3 inhibitor midostaurin has shown efficacy in patients with a low m*FLT3* allelic ratio.[38] It is possible that RTK pathway signaling in subclones can influence all leukemia cells, including neighboring cells lacking RTK pathway mutations, via paracrine effects that may include cytokines and/or stromal cells. Alternatively, RTK pathway mutations may be correlated with another factor that is causally related to resistance (eg, comutational burden), and the observed association is an epiphenomenon. In this data set, the number of comutations is associated with clinical response, but not as strongly as RTK pathway mutations.

JAK2 mutations were associated with a high CR/CRh rate (64%), with the caveat of the limited number of patients (n = 11). Although *JAK2* mutations are often classed together with other mutations affecting MAPK pathway signaling, their different pattern of response to ivosidenib treatment points to the distinct biology of *JAK2* mutations, such as STAT pathway activation, frequent ancestral status during clonal evolution, and association with prior myeloproliferative neoplasm. The number of patients is insufficient to determine whether de novo or secondary disease has a prognostic role in the context of *JAK2* mutation. Data on additional patients with *JAK2* mutations are needed to gain a more robust picture of this patient subset.

We found no significant association between clonal hierarchy and response to ivosidenib therapy, as assessed by the VAF of m*IDH1* in relation to the VAF of other co-occurring mutations. This demonstrates that mIDH1 inhibition can be efficacious even in patients with a subclonal *IDH1* mutation.

Single-cell DNA sequencing analyses uncovered bona fide co-occurring mutations at single-cell resolution, including genes of the RTK pathway (eg, *NRAS*, *KRAS*, *PTPN11*, *FLT3*), transcription factors (*RUNX1*), chromatin/epigenetic regulators (*DNMT3A*, *ASXL1*), and splicing factors (*U2AF*, *SF3B1*). These co-occurring mutations indicate functional interplay between these genes and m*IDH1*, and reflect a more complex role of m*IDH1* during leukemogenesis or maintenance of m*IDH1* AML, such as co-operation with the constitutively activated RTK pathway to promote cell proliferation, and/or cooperation with chromatin/epigenetic regulators and transcription regulators to block cell differentiation. In the majority of cases, emerging m*IDH2* is found within the same cell as m*IDH1*, indicating that m*IDH1* AML is highly "addicted" to m*IDH* and tends toward reactivating the capability to produce 2-HG. Moreover, patterns of linear and branching clonal evolution were observed with single-cell DNA sequencing, highlighting additional complexity. Single-cell DNA sequencing proved to be a powerful tool in delineating molecular outcomes for patients with m*IDH1* R/R AML.

Our findings highlight the interplay among baseline mutation profiles, response, and clonal evolution during ivosidenib therapy. The finding that the mechanism of resistance to ivosidenib is complex and polyclonal has implications for mIDH1/2 inhibitor treatment strategies, and supports the use of combination therapies or sequential treatment modifications at early relapse before overt clinical progression, rather than monotherapy with mIDH1/2 inhibitors. It will also be important to understand whether or not these patterns of resistance are replicated with combination therapies. Thorough cataloging of resistance mechanisms to targeted therapies has proven invaluable in the development of next-generation therapies, such as second- and third-generation inhibitors of BCR-ABL, EGFR, and ALK, and in the development of efficacious combination therapies such as BRAF-MEK dual inhibition in melanoma.[39] In patients with m*IDH1* AML with *FLT3*, *RAS*, or other signaling mutations, dual treatment with kinase inhibitors (FLT3 or MEK) may improve responses. In addition, dual pharmacologic inhibition of both mIDH1 and mIDH2 could potentially alleviate 2-HG restoration caused by isoform switching. Because individual patients often show multiple resistance mechanisms at relapse, combination of ivosidenib with nontargeted agents, such as intensive chemotherapy/cytotoxic therapies, hypomethylating agents, and venetoclax (BCL-2 inhibitor), may improve responses and decrease the likelihood of relapse.

Acknowledgments

The authors thank Pedro Mendez and Robert Durruthy-Durruthy (Mission Bio) for technical support of single-cell DNA sequencing analyses.

Medical writing assistance was provided by Helen Varley of Excel Medical Affairs, Horsham, United Kingdom, and funded by Agios.

Authorship

Contribution: S.C., H.W., C.D.D., E.M.S., S.d.B., G.J.R., J.K.A., A.S.M., J.W., D.A.P., A.T.F., M.S.T., H.M.K., R.M.S., L.Q., B.N., M.G., W.L., K.M., C.B., S.A.B., E.C.A., and B.W. participated in the interpretation of the translational data; S.C., H.W., E.C.A., and B.W. designed the translational studies, participated in the collection and analysis of the translational data, and drafted the manuscript; C.D.D., E.M.S., S.d.B., G.J.R., J.K.A., A.S.M., J.W., D.A.P., A.T.F., M.S.T., H.M.K., and R.M.S. participated in recruitment of patients and collection of data; Z.K. and L.D. provided data and interpretation of biochemical and structural characterization of second-site IDH1 mutations; P.N. participated in clinical sample management; G.L. oversaw the generation and collection of 2-HG data; V.Z. and H.L. participated in the statistical analyses of the translational data; H.L., M.G., and E.C.A. designed the clinical study and developed the protocol; B.W. developed and oversaw the translational science plan; and all authors contributed to the review and revision of the manuscript for important intellectual content and approved the final version for submission.

Conflict-of-interest disclosure: S.C., H.W., Z.K., L.D., B.N., P.N., G.L., V.Z., H.L., M.G., W.L., K.M., C.B., S.A.B., and B.W. are employees of and have equity ownership in Agios. C.D.D. has received honoraria and research funding from AbbVie, Agios, Celgene, and Daiichi Sankyo, and honoraria from MedImmune. E.M.S. has membership on the board of directors or advisory committee for Agios, Astellas, Celgene, Daiichi Sankyo, Genentech, Novartis, PTC Therapeutics, and Syros, and has acted as consultant for Agios. S.d.B. has acted as consultant for AbbVie, Agios, Astellas, Bayer, Celgene, Daiichi Sankyo, Forma, Janssen, Novartis, Pfizer, Pierre Fabre, Servier, and Syros; has received research funding from Agios and Forma; and is on a speaker bureau for Celgene. G.J.R. has acted as consultant or member of a data and safety monitoring committee for AbbVie, Actinium, Agios, Amphivena, Argenx, Astellas, Astex, Bayer, Celgene, Celltrion, Daiichi Sankyo, Eisai, Janssen, Jazz, MEI Pharma, Novartis, Orsenix, Otsuka, Pfizer, Roche/Genentech, Sandoz, Takeda, and Trovagene, and has received research funding from Cellectis. J.K.A. has acted as a consultant to AbbVie, Agios, Cancer Expert Now, Daiichi Sankyo, Glycomimetics, Novartis, and Theradex; is on a speaker bureau for France Foundation, PeerView, and prIME Oncology; and has received research funding to their institution from Agios, Astellas, Boehringer Ingelheim, Celgene, Fujifilm, and Genentech. A.S.M. has acted as a consultant to AbbVie, Agios, Astellas, Jazz, and PTC Therapeutics. J.W. has membership on the board of directors or advisory committee for Celgene and Pfizer, has received research funding from Takeda, and has acted as consultant and is on a speaker bureau for Jazz. D.A.P. has acted as a consultant to AbbVie, Agios, Argenx, Celgene, Celyad, Curis, Pfizer, and Servier, and has received research funding from Agios and Pfizer. A.T.F. has acted as a consultant for AbbVie, Agios, Amphivena, Astellas, Celgene, Daiichi Sankyo, Forty Seven, Jazz, Kite, NewLink Genetics, Novartis, PTC Therapeutics, Takeda, and Trovagene. M.S.T. has received research funding from AbbVie, ADC Therapeutics, BioSight, Cellerant, and Orsenix; has acted as a consultant and has membership on the board of directors or advisory committee for AbbVie, BioLineRx, Daiichi Sankyo, Delta Fly Pharma, Jazz, KAHR, Nohla, Oncolyze, Orsenix, Rigel, and Tetraphase; and holds patents or royalties with UpToDate. H.M.K. has received research funding from Ariad, Astex, Bristol Myers Squibb, Cyclacel, Daiichi Sankyo, Immunogen, Jazz, Novartis, and Pfizer and honorarium from Actinium, Immunogen, Pfizer, and Takeda. R.M.S. has acted as a consultant for AbbVie, Actinium, Agios, Amgen, Argenx, Arog, Astellas, AstraZeneca, BioLineRx, Celgene, Cornerstone Biopharma, Fujifilm, Jazz, Merck, Novartis, Ono, Orsenix, Otsuka, Pfizer, Sumitomo, and Trovagene; has received research funding from Agios, Arog, and Novartis; and is a member of a data and safety monitoring board for Argenx, Celgene, and Takeda Oncology. L.Q. has received research funding from Agios and Celgene and is on a speaker bureau for Celgene. E.C.A. was an employee of and had equity ownership in Agios at the time of the study and is currently an employee of Aprea Therapeutics.

ORCID profiles: H.W., 0000-0002-1104-1540; C.D.D., 0000-0001-9003-0390; S.d.B., 0000-0002-8126-4942; G.J.R., 0000-0002-0384-3658; D.A.P., 0000-0001-6519-4860; A.T.F., 0000-0003-4907-6447; H.M.K., 0000-0002-1908-3307; B.W., 0000-0001-9232-4456.

Correspondence: Bin Wu, Agios, Clinical Biomarkers, 88 Sidney St, Cambridge, MA 02139; e-mail: bin.wu@agios.com.

References

1. Dang L, White DW, Gross S, et al. Cancer-associated IDH1 mutations produce 2-hydroxyglutarate [published correction appears in *Nature*. 2010; 465(7300):966]. *Nature*. 2009;462(7274):739-744.
2. Ward PS, Patel J, Wise DR, et al. The common feature of leukemia-associated IDH1 and IDH2 mutations is a neomorphic enzyme activity converting alpha-ketoglutarate to 2-hydroxyglutarate. *Cancer Cell*. 2010;17(3):225-234.
3. Xu W, Yang H, Liu Y, et al. Oncometabolite 2-hydroxyglutarate is a competitive inhibitor of α-ketoglutarate-dependent dioxygenases. *Cancer Cell*. 2011; 19(1):17-30.
4. Lu C, Ward PS, Kapoor GS, et al. IDH mutation impairs histone demethylation and results in a block to cell differentiation. *Nature*. 2012;483(7390): 474-478.
5. Saha SK, Parachoniak CA, Ghanta KS, et al. Mutant IDH inhibits HNF-4α to block hepatocyte differentiation and promote biliary cancer [published correction appears in *Nature*. 2015;528(7580):152]. *Nature*. 2014;513(7516):110-114.
6. Mardis ER, Ding L, Dooling DJ, et al. Recurring mutations found by sequencing an acute myeloid leukemia genome. *N Engl J Med*. 2009;361(11): 1058-1066.

7. Patel KP, Ravandi F, Ma D, et al. Acute myeloid leukemia with *IDH1* or *IDH2* mutation: frequency and clinicopathologic features. *Am J Clin Pathol*. 2011; 135(1):35-45.

8. DiNardo CD, Ravandi F, Agresta S, et al. Characteristics, clinical outcome, and prognostic significance of IDH mutations in AML. *Am J Hematol*. 2015; 90(8):732-736.

9. Paschka P, Schlenk RF, Gaidzik VI, et al. *IDH1* and *IDH2* mutations are frequent genetic alterations in acute myeloid leukemia and confer adverse prognosis in cytogenetically normal acute myeloid leukemia with *NPM1* mutation without *FLT3* internal tandem duplication. *J Clin Oncol*. 2010;28(22): 3636-3643.

10. Feng JH, Guo XP, Chen YY, Wang ZJ, Cheng YP, Tang YM. Prognostic significance of IDH1 mutations in acute myeloid leukemia: a meta-analysis. *Am J Blood Res*. 2012;2(4):254-264.

11. Xu Q, Li Y, Lv N, et al. Correlation between isocitrate dehydrogenase gene aberrations and prognosis of patients with acute myeloid leukemia: a systematic review and meta-analysis. *Clin Cancer Res*. 2017;23(15):4511-4522.

12. Zhou KG, Jiang LJ, Shang Z, Wang J, Huang L, Zhou JF. Potential application of *IDH1* and *IDH2* mutations as prognostic indicators in non-promyelocytic acute myeloid leukemia: a meta-analysis. *Leuk Lymphoma*. 2012;53(12):2423-2429.

13. Popovici-Muller J, Lemieux RM, Artin E, et al. Discovery of AG-120 (ivosidenib): a first-in-class mutant IDH1 inhibitor for the treatment of IDH1 mutant cancers. *ACS Med Chem Lett*. 2018;9(4):300-305.

14. Yen K, Travins J, Wang F, et al. AG-221, a first-in-class therapy targeting acute myeloid leukemia harboring oncogenic *IDH2* mutations. *Cancer Discov*. 2017;7(5):478-493.

15. Tibsovo. Prescribing information. Agios Pharmaceuticals, Inc.; 2019.

16. Idhifa. Prescribing information. Celgene Corporation; 2019.

17. DiNardo CD, Stein EM, de Botton S, et al. Durable remissions with ivosidenib in *IDH1*-mutated relapsed or refractory AML. *N Engl J Med*. 2018;378(25): 2386-2398.

18. Amatangelo MD, Quek L, Shih A, et al. Enasidenib induces acute myeloid leukemia cell differentiation to promote clinical response. *Blood*. 2017;130(6): 732-741.

19. Quek L, David MD, Kennedy A, et al. Clonal heterogeneity of acute myeloid leukemia treated with the IDH2 inhibitor enasidenib. *Nat Med*. 2018;24(8): 1167-1177.

20. Harding JJ, Lowery MA, Shih AH, et al. Isoform switching as a mechanism of acquired resistance to mutant isocitrate dehydrogenase inhibition. *Cancer Discov*. 2018;8(12):1540-1547.

21. Intlekofer AM, Shih AH, Wang B, et al. Acquired resistance to IDH inhibition through trans or cis dimer-interface mutations. *Nature*. 2018;559(7712): 125-129.

22. Döhner H, Estey E, Grimwade D, et al. Diagnosis and management of AML in adults: 2017 ELN recommendations from an international expert panel. *Blood*. 2017;129(4):424-447.

23. Kluk MJ, Lindsley RC, Aster JC, et al. Validation and implementation of a custom next-generation sequencing clinical assay for hematologic malignancies. *J Mol Diagn*. 2016;18(4):507-515.

24. Molenaar RJ, Thota S, Nagata Y, et al. Clinical and biological implications of ancestral and non-ancestral *IDH1* and *IDH2* mutations in myeloid neoplasms. *Leukemia*. 2015;29(11):2134-2142.

25. Papaemmanuil E, Gerstung M, Bullinger L, et al. Genomic classification and prognosis in acute myeloid leukemia. *N Engl J Med*. 2016;374(23): 2209-2221.

26. Center for Drug Evaluation and Research. NDA multidisciplinary review and evaluation: ivosidenib. Available at: www.accessdata.fda.gov/drugsatfda_docs/nda/2018/211192Orig1s000MultidisciplineR.pdf. Accessed 21 February 2020.

27. Kohanbash G, Carrera DA, Shrivastav S, et al. Isocitrate dehydrogenase mutations suppress STAT1 and CD8+ T cell accumulation in gliomas. *J Clin Invest*. 2017;127(4):1425-1437.

28. Ugele I, Cárdenas-Conejo ZE, Hammon K, et al. D-2-hydroxyglutarate and L-2-hydroxyglutarate inhibit IL-12 secretion by human monocyte-derived dendritic cells. *Int J Mol Sci*. 2019;20(3):E742.

29. Brauburger K, Burckhardt G, Burckhardt BC. The sodium-dependent di- and tricarboxylate transporter, NaCT, is not responsible for the uptake of D-, L-2-hydroxyglutarate and 3-hydroxyglutarate into neurons. *J Inherit Metab Dis*. 2011;34(2):477-482.

30. Bunse L, Pusch S, Bunse T, et al. Suppression of antitumor T cell immunity by the oncometabolite (R)-2-hydroxyglutarate. *Nat Med*. 2018;24(8): 1192-1203.

31. McMahon CM, Ferng T, Canaani J, et al. Clonal selection with RAS pathway activation mediates secondary clinical resistance to selective FLT3 inhibition in acute myeloid leukemia. *Cancer Discov*. 2019;9(8):1050-1063.

32. Sexauer A, Perl A, Yang X, et al. Terminal myeloid differentiation in vivo is induced by FLT3 inhibition in FLT3/ITD AML. *Blood*. 2012;120(20):4205-4214.

33. McMahon CM, Canaani J, Rea B, et al. Gilteritinib induces differentiation in relapsed and refractory *FLT3*-mutated acute myeloid leukemia. *Blood Adv*. 2019;3(10):1581-1585.

34. Flavahan WA, Drier Y, Liau BB, et al. Insulator dysfunction and oncogene activation in IDH mutant gliomas. *Nature*. 2016;529(7584):110-114.

35. Zhu H, Zhang Y, Chen J, et al. IDH1 R132H mutation enhances cell migration by activating AKT-mTOR signaling pathway, but sensitizes cells to 5-FU treatment as NADPH and GSH are reduced. *PLoS One*. 2017;12(1):e0169038.

36. Carbonneau M, Gagné LM, Lalonde ME, et al. The oncometabolite 2-hydroxyglutarate activates the mTOR signalling pathway. *Nat Commun*. 2016;7: 12700.

37. Zhang Y, Kwok-Shing Ng P, Kucherlapati M, et al. A pan-cancer proteogenomic atlas of PI3K/AKT/mTOR pathway alterations. *Cancer Cell*. 2017;31(6): 820-832.

38. Stone RM, Mandrekar SJ, Sanford BL, et al. Midostaurin plus chemotherapy for acute myeloid leukemia with a *FLT3* mutation. *N Engl J Med*. 2017; 377(5):454-464.

39. Robert C, Karaszewska B, Schachter J, et al. Improved overall survival in melanoma with combined dabrafenib and trametinib. *N Engl J Med*. 2015; 372(1):30-39.

40. Jones S, Ahmet J, Ayton K, et al. Discovery and optimization of allosteric inhibitors of mutant isocitrate dehydrogenase 1 (R132H IDH1) displaying activity in human acute myeloid leukemia cells. *J Med Chem*. 2016;59(24):11120-11137.